UDC 535.42:537.8

S. S. Apostolov[1, 2], D. A. Iakushev[1], N. M. Makarov[1, 3], A. A. Shmat'ko[2], and V. A. Yampol'skii[1, 2]
[1]*A. Ya. Usikov Institute for Radiophysics and Electronics NASU, 61085 Kharkov, Ukraine*
[2]*V. N. Karazin Kharkov National University, 61077, Kharkov, Ukraine*
[3]*Benemérita Universidad Autónoma de Puebla, Puebla, Pue. 72000, México*
E-mail: yam@ire.kharkov.ua

TERAHERTZ TRANSVERSE-MAGNETIC-POLARIZED WAVES LOCALIZED ON A LAYERED SUPERCONDUCTOR DEFECT IN PHOTONIC CRYSTALS

We theoretically study eigenstates of electromagnetic field inside a one-dimensional photonic crystal containing a defect slab of layered superconductor. Basing on the transfer matrix formalism along with the electrodynamics of Josephson plasma, we obtain the dispersion relations describing the THz electromagnetic modes localized on defect. We consider both symmetric and antisymmetric configuration of defect in photonic crystal. The comparison of the dispersion spectra of the localized states for the layered-superconducting defect and the pure insulating defect reveals the features of the studied system. Fig. 3. Ref.: 14 title.

Key words: photonic crystal, transfer matrix, layered superconductor.

During recent years, layered superconductors attract great attention due to their special electrodynamic properties. These media are composed of superconducting films with thicknesses ~ 0.2 nm, which are separated by thicker dielectric slabs with thicknesses ~ 1.5 nm and dielectric constant ~ 16. As was shown in experiments [1, 2], the superconducting layers are electrodynamically coupled because of the intrinsic Josephson effect giving rise to emerging a peculiar type of plasma, so called Josephson plasma, in such strongly anisotropic materials.

The anisotropy results in the existence of the specific electromagnetic excitations in such layered media, known as the Josephson plasma waves (JPWs), see, e. g. [3, 4] and references therein. A distinctive feature of the layered superconductors is that, due to the Josephson effect, the weak current across the layers is formed, whereas the strong electric current flowing along the layers has the same origin as in bulk superconductors. It is important that the typical frequencies of JPWs belong to the terahertz (THz) frequency range. This makes layered superconductors to be promising materials for various optical applications, see, e. g. [5].

In works [6, 7] it was theoretically demonstrated that the surface Josephson plasma waves (SJPWs) can propagate along interfaces between layered superconductors and vacuum, similarly to the surface plasmon-polaritons in the case of usual plasmas. It is interesting that the Josephson plasma represents a medium in which some famous electromagnetic phenomena have been observed. Among them one can mention the Wood anomalies and the Anderson localization. Thus, the excitation of SJPWs give rise to various resonant phenomena [7–9] that are similar to the Wood anomalies well-known in optics, see, e. g. [10–12]. A noticeable difference with respect to usual plasmas is that SJPWs can propagate with frequencies not only below the Josephson plasma frequency ω_J but also above it [7]. As was shown in [13], the phenomena similar to the Anderson localization and the formation of a transparency window for THz electromagnetic waves can be observed in layered superconductors with randomly-fluctuating value of the maximum Josephson current. Also it is important to mention that the Josephson plasma can have properties intrinsic to the left-handed media. In particular, one can observe a negative refractive index for THz waves at the boundaries of layered superconductors [7, 14].

Because of unusual electromagnetic properties of layered superconductors, it is of interest to examine photonics of various structures containing components made of layered superconductors. In the present work we analyze photonic spectrum of one-dimensional periodic photonic crystal with an extra slab of layered superconductor.

1. Problem formulation. We explore eigenstates of the electromagnetic field inside a one-dimensional dielectric photonic crystal with a defect. The unit cell of the photonic crystal is composed of two non-magnetic dielectric layers with thicknesses d_1 and d_2, see Fig. 1. The size of the whole unit cell is $d = d_1 + d_2$. The permittivities of the layers with sizes d_1 and d_2 are ε_1 and ε_2, respectively.

The defect is an extra layer of thickness D which can be inserted between two basic layers of the photonic-crystal unit-cell or replace one of them (see, respectively, upper and lower panel of Fig. 1). The defect consists of alternating slabs of dielectric and superconductor arranged orthogonally to the layers of photonic crystal and occupies the spatial region $0 < x < D$.

The interaction of an electromagnetic wave of frequency ω with the defect of layered superconductor can be described by the effective permittivity tensor that has the following components

$$\varepsilon_{xx}(\Omega)=\varepsilon_{yy}(\Omega)=\varepsilon\left(1-\frac{\gamma^2}{\Omega^2}\right),\quad \varepsilon_{zz}(\Omega)=\varepsilon\left(1-\frac{1}{\Omega^2}\right), \tag{1}$$

where Ω is the wave frequency normalized to the Josephson plasma frequency ω_J,

$$\Omega=\omega/\omega_J, \tag{2}$$

$\omega_J=(8\pi e J_c d_i/\hbar\varepsilon)^{1/2}$; J_c is the maximal Josephson current density; ε and d_i are the dielectric constant and the thickness of the insulator components of layered super conductor, respectively; e is the elementary charge. In addition, the electrodynamics of the layered superconductor is characterized by the London penetration depth λ_c along the superconducting layers, $\lambda_c=c/\omega_J\varepsilon^{1/2}$, and the London penetration depths λ_{ab} across the layers. In the paper we assume $\lambda_{ab}<<\lambda_c$, e. g. the anisotropy parameter $\gamma=\lambda_c/\lambda_{ab}$ is great, $\gamma>>1$.

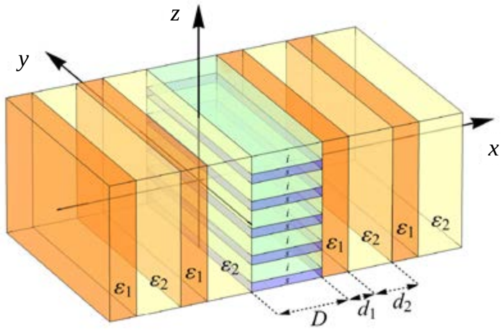

a)

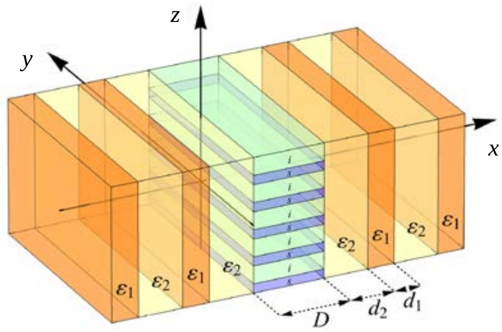

b)

Fig. 1. (Color Online) A sketch of the structure. Upper and lower panels demonstrate the non-symmetric (a) and symmetric (b) setups, correspondingly

In the present study we focus on *TM*-polarized electromagnetic waves. Their electric $\vec{E}$ and magnetic $\vec{H}$ components are determined by the following expressions,

$$\begin{aligned}\vec{E}(x,z,t)&=\{E_x(x),0,E_z(x)\}\exp[i(k_z z-\omega t)],\\ \vec{H}(x,z,t)&=\{0,H_y(x),0\}\exp[i(k_z z-\omega t)],\end{aligned} \tag{3}$$

where the z-component k_z of the total wave vector $\vec{k}$ an independent parameter of the problem characterizing the wave propagation angle with respect to the stratification of the dielectric photonic crystal.

II. Propagation matrices of the system

A. Propagation matrix of the photonic crystal unit-cell. The electric and magnetic fields on the opposite boundaries of the photonic crystal unit-cells are related by

$$\begin{pmatrix}H_y(x=(n+1)d)\\ E_z(x=(n+1)d)\end{pmatrix}=\hat{\mathbf{M}}\begin{pmatrix}H_y(x=nd)\\ E_z(x=nd)\end{pmatrix} \tag{4}$$

with n being the unit-cell number and d being its size, $d=d_1+d_2$. The elements of the propagation matrix $\hat{\mathbf{M}}$ are given by

$$\begin{aligned}M_{11}&=\cos\varphi_1\cos\varphi_2-\frac{\varepsilon_2 k_{1x}}{\varepsilon_1 k_{2x}}\sin\varphi_1\sin\varphi_2,\\ M_{12}&=-i\frac{\omega\varepsilon_1}{ck_{1x}}\sin\varphi_1\cos\varphi_2-i\frac{\omega\varepsilon_2}{ck_{2x}}\sin\varphi_2\cos\varphi_1,\\ M_{21}&=-i\frac{ck_{1x}}{\omega\varepsilon_1}\sin\varphi_1\cos\varphi_2-i\frac{ck_{2x}}{\omega\varepsilon_2}\sin\varphi_2\cos\varphi_1,\\ M_{22}&=\cos\varphi_1\cos\varphi_2-\frac{\varepsilon_1 k_{2x}}{\varepsilon_2 k_{1x}}\sin\varphi_1\sin\varphi_2.\end{aligned} \tag{5}$$

Here

$$\begin{aligned}&\varphi_1=k_{1x}d_1,\quad \varphi_2=k_{2x}d_2,\\ &k_{1x}=\sqrt{k_0^2\varepsilon_1-k_z^2},\quad k_{2x}=\sqrt{k_0^2\varepsilon_2-k_z^2},\end{aligned} \tag{6}$$

and $k_0=\omega/c$.

In the absence of defect, due to the translation symmetry of photonic crystal, the electric and magnetic fields, in addition to Eq. (4), should satisfy the Bloch relation,

$$\begin{pmatrix}H_y(x=(n+1)d)\\ E_z(x=(n+1)d)\end{pmatrix}=\exp(\pm i\mu_B)\begin{pmatrix}H_y(x=nd)\\ E_z(x=nd)\end{pmatrix}, \tag{7}$$

where μ_B is the Bloch phase associated with the Bloch wave number κ as $\mu_B=\kappa d$.

Equations (4) and (7) lead to dispersion relation $2\cos\mu_B=M_{11}+M_{22}$, which, after substitution of the matrix elements, transforms to the well known dispersion relation of dielectric bi-layer array,

$$\cos\mu_B=\cos\varphi_1\cos\varphi_2-\frac{1}{2}\left(\frac{\varepsilon_2 k_{1x}}{\varepsilon_1 k_{2x}}+\frac{\varepsilon_1 k_{2x}}{\varepsilon_2 k_{1x}}\right)\sin\varphi_1\sin\varphi_2. \tag{8}$$

Note that the wave numbers k_{1x}, k_{2x} and phase shifts φ_1, φ_2, which are given by Eqs. (6), can be either strictly real or strictly imaginary. Therefore the right-hand side of Eq. (8) and, as a consequence, $\cos\mu_B$ are always of strictly real values. Thus, equation (8) has an infinite number of solutions for the Bloch phase μ_B. If we confine them within the first Brillouin zone ($-\pi \le \mathrm{Re}\,\mu_B \le \pi$), then μ_B is real (for $|\cos\mu_B| \le 1$), pure imaginary (for $\cos\mu_B > 1$), or complex with the real part equal $\pm\pi$ (for $\cos\mu_B < -1$).

B. Propagation matrix of superconducting defect. In this subsection we concentrate our attention on the case when the *z*-projection of the wave vector $k_z \sim \omega / c$ and the wave frequency $\omega \sim \omega_J$. Due to these restrictions, in the Maxwell equations, the terms of the order of γ^2 originated from the effective permittivity tensor (1), prevail over the others. Solving the Maxwell equations in the layered superconductor we obtain the tangential components of the electromagnetic field in the following form

$$E_z(\xi) = -\frac{i\Omega}{\sqrt{\varepsilon}}(C_1 e^{i\tilde{\Omega}\xi} + C_2 e^{-i\tilde{\Omega}\xi}),$$
$$H_y(\xi) = i\tilde{\Omega}(C_1 e^{i\tilde{\Omega}\xi} - C_2 e^{-i\tilde{\Omega}\xi}), \tag{9}$$

where the normalized *x*-projection of the wave vector is denoted as

$$\tilde{\Omega} = \sqrt{\Omega^2 - 1}. \tag{10}$$

Here we introduced the dimensionless coordinate ξ and the normalized thickness δ of the layered-superconductor slab,

$$\xi = \frac{x}{\lambda_c}, \quad \delta = \frac{D}{\lambda_c} >> 1. \tag{11}$$

In correspondence with Eq. (9), the propagation matrix $\hat{\mathbf{M}}^{(s)}$ for the defect of layered superconductor of thickness *D*, relating the electric and magnetic fields on the opposite boundaries of the defect,

$$\begin{pmatrix} H_y(x=D) \\ E_z(x=D) \end{pmatrix} = \hat{\mathbf{M}}^{(s)} \begin{pmatrix} H_y(x=0) \\ E_z(x=0) \end{pmatrix}, \tag{12}$$

can be written as

$$\hat{\mathbf{M}}^{(s)} = \begin{pmatrix} \cos(\delta\tilde{\Omega}) & (\sqrt{\varepsilon}\tilde{\Omega}/i\Omega)\sin(\delta\tilde{\Omega}) \\ (\Omega/i\sqrt{\varepsilon}\tilde{\Omega})\sin(\delta\tilde{\Omega}) & \cos(\delta\tilde{\Omega}) \end{pmatrix}, \tag{13}$$

For the symmetric setup it is convenient to assume that the localized states are symmetric with respect to the center of the defect, $x = D/2$. In this geometry the fields in the center, $x = D/2$, are related to the fields at the interface, $x = D$, by the propagation matrix $\hat{\mathbf{M}}^{(s/2)}$,

$$\begin{pmatrix} H_y(x=D) \\ E_z(x=D) \end{pmatrix} = \hat{\mathbf{M}}^{(s/2)} \begin{pmatrix} H_y(x=D/2) \\ E_z(x=D/2) \end{pmatrix}. \tag{14}$$

The elements of matrix $\hat{\mathbf{M}}^{(s/2)}$ are analogous to Eq. (13), but with δ changed by $\delta/2$,

$$\hat{\mathbf{M}}^{(s/2)} = \begin{pmatrix} \cos(\delta\tilde{\Omega}/2) & (\sqrt{\varepsilon}\tilde{\Omega}/i\Omega)\sin(\delta\tilde{\Omega}/2) \\ (\Omega/i\sqrt{\varepsilon}\tilde{\Omega})\sin(\delta\tilde{\Omega}/2) & \cos(\delta\tilde{\Omega}/2) \end{pmatrix}. \tag{15}$$

3. The localized states

A. Non-symmetric setup. Here we derive the dispersion relation for the states localized on the defect for non-symmetric setup (see panel (a) in Fig. 1). To this end, we assume that the frequency Ω is within a spectral gap of the photonic crystal without defect. In this case, in the representation of extended Brillouin zones, the Bloch phase μ_B, see Eq. (8) and speculations after, has the imaginary part and its real part equals $m\pi$ with integer *m*, $\mu_B = m\pi + i\psi$, $\psi > 0$. Then the eigenvalues $\exp(\pm i\mu_B)$ of the propagation matrix (5) are $(-1)^m \exp(\mp\psi)$ and their absolute values are not equal to one.

To proceed further, we need to introduce the Jordan decomposition of the propagation matrix, $\hat{\mathbf{M}} = \hat{\mathbf{S}}^{-1}\hat{\mathbf{\Lambda}}\hat{\mathbf{S}}$ where the eigenmatrix $\hat{\mathbf{\Lambda}}$ and the transformation matrix $\hat{\mathbf{S}}$ read

$$\hat{\mathbf{\Lambda}} = \begin{pmatrix} (-1)^m e^{-\psi} & 0 \\ 0 & (-1)^m e^{\psi} \end{pmatrix},$$
$$\hat{\mathbf{S}} = \begin{pmatrix} M_{11} - (-1)^m e^{\psi} & M_{12} \\ (-1)^m e^{-\psi} - M_{11} & -M_{12} \end{pmatrix}. \tag{16}$$

If we know the fields at the right surface of the defect (at $x = D$), then, by applying *N* times the propagation matrix $\hat{\mathbf{M}}$ to them, we can get the fields on the right interface of the *N*-th unit cell (at $x = D + Nd$),

$$\begin{pmatrix} H_y(x=D+Nd) \\ E_z(x=D+Nd) \end{pmatrix} = \hat{\mathbf{M}}^N \begin{pmatrix} H_y(x=D) \\ E_z(x=D) \end{pmatrix} =$$
$$= (-1)^{mN}\hat{\mathbf{S}}^{-1} \begin{pmatrix} e^{-N\psi} & 0 \\ 0 & e^{N\psi} \end{pmatrix} \hat{\mathbf{S}} \begin{pmatrix} H_y(x=D) \\ E_z(x=D) \end{pmatrix}. \tag{17}$$

In the limit $N \to \infty$ the fields at $x = D + Nd$ tends to zero because they are assumed to be localized on the defect. So, we get

$$\begin{pmatrix} 0 & 0 \\ 0 & 1 \end{pmatrix} \hat{\mathbf{S}} \begin{pmatrix} H_y(x=D) \\ E_z(x=D) \end{pmatrix} = 0, \tag{18}$$

that is

$$\frac{H_y(x=D)}{E_z(x=D)} = \frac{M_{12}}{(-1)^m e^{-\psi} - M_{11}}. \tag{19}$$

Analogously, the fields on the left surface of the defect (at $x = 0$) can be expressed via the fields on the surface of the $(-N)$-th cell (at $x = -Nd$),

$$\begin{pmatrix} H_y(x=-Nd) \\ E_z(x=-Nd) \end{pmatrix} = \hat{\mathbf{M}}^{-N} \begin{pmatrix} H_y(x=0) \\ E_z(x=0) \end{pmatrix} = \\ = (-1)^{mN} \hat{\mathbf{S}}^{-1} \begin{pmatrix} e^{N\psi} & 0 \\ 0 & e^{-N\psi} \end{pmatrix} \hat{\mathbf{S}} \begin{pmatrix} H_y(x=0) \\ E_z(x=0) \end{pmatrix}. \tag{20}$$

In the limit $N \to \infty$ the fields at $x = -Nd$ tends to zero and we get

$$\begin{pmatrix} 1 & 0 \\ 0 & 0 \end{pmatrix} \hat{\mathbf{S}} \begin{pmatrix} H_y(x=0) \\ E_z(x=0) \end{pmatrix} = 0, \tag{21}$$

that is

$$\frac{H_y(x=0)}{E_z(x=0)} = \frac{M_{12}}{(-1)^m e^{\psi} - M_{11}}. \tag{22}$$

With the use of equations (19), (22) and (12), taking into account that $M_{11}^{(s)} = M_{22}^{(s)}$, we readily derive the complemental to (8), dispersion relation

$$\sin\mu_B = -i\frac{M_{12}M_{21}^{(s)} + M_{21}M_{12}^{(s)}}{2M_{11}^{(s)}}. \tag{23}$$

By employing the explicit expressions (13) for the propagation matrix of the layered superconductor and that the Bloch phase are determined as $\mu_B = m\pi + i\psi$, this dispersion relation can be rewritten as follows

$$\frac{(-1)^m i}{2\sinh\psi}\left[\frac{\sqrt{\varepsilon}\tilde{\Omega}}{\Omega}M_{21} + \frac{\Omega}{\sqrt{\varepsilon}\tilde{\Omega}}M_{12}\right] = \cot(\delta\tilde{\Omega}). \tag{24}$$

Note that at the same values of the Bloch phase $\mu_B = m\pi + i\psi$, the initial dispersion relation (8) is transformed to

$$(-1)^m \cosh\psi = \frac{1}{2}(M_{11} + M_{22}), \tag{25}$$

and the elements of the propagation matrix $\hat{\mathbf{M}}$ defined in Eqs. (5) can be presented in dimensionless variables as

$$\begin{aligned} M_{11} &= \cos\varphi_1\cos\varphi_2 - \frac{\rho_2\kappa_1}{\rho_1\kappa_2}\sin\varphi_1\sin\varphi_2, \\ M_{12} &= \frac{\Omega\sqrt{\varepsilon}}{i}\left(\frac{\rho_1}{\kappa_1}\sin\varphi_1\cos\varphi_2 + \frac{\rho_2}{\kappa_2}\sin\varphi_2\cos\varphi_1\right), \\ M_{21} &= \frac{-i}{\Omega\sqrt{\varepsilon}}\left(\frac{\kappa_1}{\rho_1}\sin\varphi_1\cos\varphi_2 + \frac{\kappa_2}{\rho_2}\sin\varphi_2\cos\varphi_1\right), \\ M_{22} &= \cos\varphi_1\cos\varphi_2 - \frac{\rho_1\kappa_2}{\rho_2\kappa_1}\sin\varphi_1\sin\varphi_2. \end{aligned} \tag{26}$$

Here

$$\varphi_i = \kappa_i\delta_i, \quad \kappa_i = k_{ix}\lambda_c = \sqrt{\Omega^2\rho_i - \kappa^2}, \\ \delta_i = \frac{d_i}{\lambda_c}, \quad \kappa = k_z\lambda_c, \quad \rho_i = \frac{\varepsilon_i}{\varepsilon}, \quad i = 1,2. \tag{27}$$

Applying the expressions (26) for the propagation matrix $\hat{\mathbf{M}}$ in Eqs. (24) and (25), we finally get the following set of the dispersion relations

$$\left(\frac{\kappa_1\tilde{\Omega}}{\rho_1\Omega^2} + \frac{\rho_1\Omega^2}{\kappa_1\tilde{\Omega}}\right)\sin\varphi_1\cos\varphi_2 + \\ + \left(\frac{\kappa_2\tilde{\Omega}}{\rho_2\Omega^2} + \frac{\rho_2\Omega^2}{\kappa_2\tilde{\Omega}}\right)\sin\varphi_2\cos\varphi_1 = \\ = 2(-1)^m \sinh\psi\cot(\delta\tilde{\Omega}), \tag{28}$$
$$(-1)^m\cosh\psi = \cos\varphi_1\cos\varphi_2 - \\ -\frac{1}{2}\left(\frac{\rho_2\kappa_1}{\rho_1\kappa_2} + \frac{\rho_1\kappa_2}{\rho_2\kappa_1}\right)\sin\varphi_1\sin\varphi_2,$$

where $\psi > 0$ and m is integer.

B. Symmetric setup. Here we derive the dispersion relation for the states localized on the defect for symmetric setup (see panel (b) in Fig. 1).

As we have already calculated above, the fields on the right interface of the defect are related as

$$\frac{H_y(x=D)}{E_z(x=D)} = \frac{M_{12}}{(-1)^m e^{-\psi} - M_{11}}. \tag{29}$$

In the case when the localized states are symmetric with respect to the center $x = D/2$ of the defect, there are two types of the states, specifically, with symmetric or antisymmetric electric field, i. e.

$$H_y(x = D/2) = 0 \quad \text{or} \quad E_z(x = D/2) = 0. \tag{30}$$

The fields in the center $x = D/2$ are related to the fields at the interface, $x = D$, by the propagation matrix $\hat{\mathbf{M}}^{(s/2)}$ given by Eq. (15). Therefore, the dispersion relation for symmetric or antisymmetric state, respectively, reads

$$\frac{M_{12}}{M_{11} - (-1)^m e^{-\psi}} = -\begin{cases} M_{12}^{(s/2)}/M_{22}^{(s/2)}, \\ M_{11}^{(s/2)}/M_{21}^{(s/2)}. \end{cases} \tag{31}$$

Using Eqs. (15), this dispersion relation can be rewritten as

$$\frac{i(\Omega/\sqrt{\varepsilon}\tilde{\Omega})M_{12}}{M_{11} - e^{im\pi-\psi}} = \begin{cases} -\tan(\delta\tilde{\Omega}/2), \\ \cot(\delta\tilde{\Omega}/2), \end{cases} \tag{32}$$

for symmetric and antisymmetric localized states, respectively.

In the dimensionless variables, with the use of Eqs. (26) and (27), Eq. (32) together with Eq. (8) results in the required set of two dispersion relations,

$$\frac{\frac{\Omega^2}{\tilde{\Omega}}\left(\frac{\rho_1}{\kappa_1}\cot\varphi_2 + \frac{\rho_2}{\kappa_2}\cot\varphi_1\right)}{\frac{1}{2}\left(\frac{\rho_1\kappa_2}{\rho_2\kappa_1} - \frac{\rho_2\kappa_1}{\rho_1\kappa_2}\right) + \frac{(-1)^m\sinh\psi}{\sin\varphi_1\sin\varphi_2}} = \begin{cases} -\tan\frac{\delta\tilde{\Omega}}{2}, \\ \cot\frac{\delta\tilde{\Omega}}{2}, \end{cases}$$
$$(-1)^m\cosh\psi = \cos\varphi_1\cos\varphi_2 - \\ -\frac{1}{2}\left(\frac{\rho_2\kappa_1}{\rho_1\kappa_2} + \frac{\rho_1\kappa_2}{\rho_2\kappa_1}\right)\sin\varphi_1\sin\varphi_2, \tag{33}$$

for symmetric and antisymmetric localized states, respectively.

C. Analysis of dispersion equations. Figure 2 shows the dispersion curves of the photonic crystal with the defect of the layered superconductor for the non-symmetric setup, Eqs. (28), and the symmetric setup, Eqs. (33). The photonic crystal consists of the two alternating layers of the silica glass ($\varepsilon_1 = 3.8$) and teflon ($\varepsilon_2 = 2.04$) with equal thicknesses, $d_1 = = d_2 = 5\lambda_c = 2 \cdot 10^{-2}$ cm. The superconducting defect of thickness $d = 3\lambda_c = 1.2 \cdot 10^{-2}$ cm is made from $Bi_2Sr_2CaCu_2O_{8+\delta}$, whose insulating layers possess dielectric constant $\varepsilon = 16$. The rest of the characteristic parameters is $\omega_J / 2\pi = 0.3$ THz, $\lambda_{ab} = 2\,000$ Å, $\lambda_c = 4 \cdot 10^{-3}$ cm. The solid curves describe the electromagnetic localized states in the non-symmetric setup, while the dotted and dashed curves present the symmetric and antisymmetric localized states, correspondingly, in the symmetric setup. The gray-filled areas corresponds to the spectral gaps of the photonic crystal without defect. Two straight lines show the light lines: $\omega = ck_z / \sqrt{\varepsilon_1}$ of the silica glass (solid line) and $\omega = ck_z / \sqrt{\varepsilon_2}$ of teflon (dashed line).

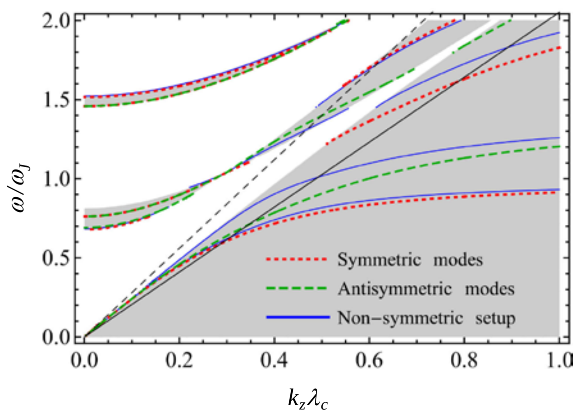

Fig. 2. (Color Online) Dispersion curves of the localized states in the photonic crystal with the defect of the layered superconductor for the non-symmetric setup (the solid curves) and the symmetric setup (the dotted and dashed curves for the symmetric and antisymmetric localized states, correspondingly)

To emphasize the features of the studied localized states, we compare the dispersion spectra for the layered-superconductor defect and the pure insulating defect. The propagation matrix $\hat{\mathbf{M}}^{(d)}$ of the insulating defect with thickness D and dielectric constant ε can be written in the following form,

$$\hat{\mathbf{M}}^{(d)} = = \begin{pmatrix} \cos(\delta\tilde{\Omega}) & (\sqrt{\varepsilon}\Omega / i\tilde{\Omega})\sin(\delta\tilde{\Omega}) \\ (\tilde{\Omega}/i\sqrt{\varepsilon}\Omega)\sin(\delta\tilde{\Omega}) & \cos(\delta\tilde{\Omega}) \end{pmatrix}, \qquad (34)$$

where

$$\tilde{\Omega} = \sqrt{\Omega^2 - \kappa^2} \qquad (35)$$

in contrast to Eq. (10). This matrix has the similar structure as the propagation matrix for the layered-superconductor defect, Eq. (13), but the difference in κ-dependence of $\tilde{\Omega}$ influences the dispersion curves qualitatively. This difference appears due to the strong anisotropy of the effective permittivity tensor of layered superconductor.

Figure 3 shows the dispersion curves of the photonic crystal with the defects of the layered superconductor (solid curves) and of the pure insulator (dashed curves) in the non-symmetric setup. The parameters of the layer-superconductor defect are the same as for Fig. 2 and the parameters of the insulating defect are thickness $d = 3\lambda_c$ and dielectric constant $\varepsilon = 16$.

Besides the quantitative differences between curves there is the essential difference. It is easy to see that for the first type of defect the dispersion curves become nearly horizontal for sufficiently large κ, while the second type of defect produces tilted up curves growing nearly as $\Omega = \kappa$. Thereby the states localized on the superconducting defect can possess sufficiently large z-projection of the wave vector, while sufficiently small frequency.

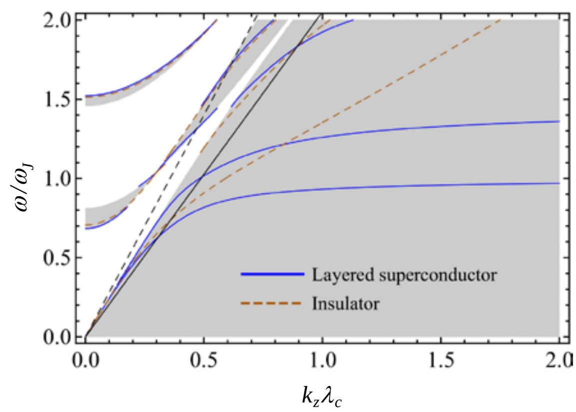

Fig. 3. (Color Online) Dispersion curves of the localized states in the photonic crystal with the defects of the layered superconductor (the solid curves) and the pure insulator (the dashed curves) for the non-symmetric setup

Conclusions. We have considered problem of eigenstates of the electromagnetic field inside photonic crystal with the defect composed of the layered superconductor. We have analyzed the cases of both symmetric and non-symmetric configurations of the defect in the photonic crystal. We have obtained the dispersion relations that describe the photonic spectrum of the localized electromagnetic waves. The dispersion relations have been analyzed numerically, compared to the case of the pure insulating defect, and defined the qualitative differences. Namely, the states localized on the superconducting defect can propagate with sufficiently large *z*-projection of the wave vector, while sufficiently small frequency.

Acknowledgements. N. M. Makarov acknowledges partial support from the CONACYT (México).

References

1. *Intrinsic* Josephson effects in $Bi_2Sr_2CaCu_2O_8$ single crystals / R. Kleiner, F. Steinmeyer, G. Kunkel, P. Müller // Phys. Rev. Lett. – 1992. – 68, N 15. – P. 2394–2397.
2. *Kleiner R.* Intrinsic Josephson effects in high-Tc superconductors / R. Kleiner, P. Müller // Phys. Rev. B. – 1994. – 49, N 2. – P. 1327–1341.
3. *Terahertz* Josephson plasma waves in layered superconductors: spectrum generation nonlinear and quantum phenomena / S. Savel'ev, V. A. Yampol'skii, A. L. Rakhmanov, F. Nori // Rep. Prog. Phys. – 2010. – 73, N 2. – P. 026501 (49 p.)
4. *Hu X.* Phase dynamics in a stack of inductively coupled intrinsic Josephson junctions and terahertz electromagnetic radiation / X. Hu, S.-Z. Lin // Supercond. Sci. Technol. – 2010. – 23, N 5. – P. 053001 (7 p.).
5. *Emission* of Coherent THz Radiation from Superconductors / L. Ozyuzer, A. E. Koshelev, C. Kurter et al. // Science. – 2007. – 318, N 5854. – P. 1291–1293.
6. *Savel'ev S.* Surface Josephson Plasma Waves in Layered Superconductors / S. Savel'ev, V. Yampol'skii, and F. Nori // Phys. Rev. Lett. – 2005. – 95, N 18. – P. 187002 (4 p.).
7. *Surface* Josephson Plasma Waves in Layered Superconductors above the Plasma Frequency: Evidence for a Negative Index of Refraction / V. A. Golick, D. V. Kadygrob, V. A. Yampolskii et al. // Phys. Rev. Lett. – 2010. – 104, N 18. – P. 187003 (4 p).
8. *Excitation* of surface Josephson plasma waves in layered superconductors / V. A. Yampol'skii, A. V. Kats, M. L. Nesterov et al. // Phys. Rev. B – 2007. – 76, N 22. – P. 224504 (7 p).
9. *Enhanced* transmission of terahertz radiation through a periodically modulated slab of layered super-conductor / D. V. Kadygrob, N. M. Makarov, F. Perez-Rodriguez et al. // New J. Phys. – 2013. – 15, N 2. – P. 023040 (9 p.).
10. *Agranovich V. M.* Surface Polaritons: Electromagnetic Waves at Surfaces & Interfaces / V. M. Agranovich, D. L. Mills (eds.) – Amsterdam: North-Holland Publishing Company, 1982. – 717 p.
11. *Raether H.* Surface plasmons on smooth and rough surfaces and on gratings / H. Raether. – N. Y.: Springer-Verlag, 1988. – 136 p.
12. *Petit R.* Electromagnetic Theory of Gratings / R. Petit. – Berlin: Springer, 1980. – 284 p.
13. *Controlled* terahertz frequency response and transparency of Josephson chains and superconducting multilayers / V. A. Yampolskii, S. Savelev, O. V. Usatenko et al. // Phys. Rev. B. – 2010. – 75, N 1. – P. 014527 (7 p.).
14. *Layered* superconductors as negative-refractive-index metamaterials / A. L. Rakhmanov, V. A. Yampol'skii, J. A. Fan et al. // Phys. Rev. B. – 2010. – 81, N 7. – P. 075101 (6 p.).

Рукопись поступила 17.10.2016.

С. С. Апостолов, Д. А. Якушев, Н. М. Макаров,
А. А. Шматько, В. А. Ямпольский

ТЕРАГЕРЦЕВЫЕ *ТМ*-ВОЛНЫ, ЛОКАЛИЗОВАННЫЕ НА ДЕФЕКТЕ ИЗ СЛОИСТОГО СВЕРХПРОВОДНИКА В ФОТОННОМ КРИСТАЛЛЕ

Теоретически исследованы собственные состояния электромагнитного поля в одномерном фотонном кристалле, содержащем дефектную пластину из слоистого сверхпроводника. Основываясь на методе трансфер-матрицы, с использованием электродинамики джозефсоновской плазмы, получены дисперсионные соотношения, описывающие терагерцевые электромагнитные моды, локализованные на дефекте. Рассмотрены симметричная и антисимметричная конфигурации дефекта в фотонном кристалле. Сравнение дисперсионных спектров локализованных состояний для сверхпроводящего и диэлектрического дефектов позволяет выявить особенности изучаемой системы.

Ключевые слова: фотонный кристалл, трансфер-матрица, слоистый сверхпроводник.

С. С. Апостолов, Д. О. Якушев, Н. М. Макаров,
А. А. Шматько, В. О. Ямпольський

ТЕРАГЕРЦОВІ *ТМ*-ХВИЛІ, ЛОКАЛІЗОВАНІ НА ДЕФЕКТІ З ШАРУВАТОГО НАДПРОВІДНИКА У ФОТОННОМУ КРИСТАЛІ

Теоретично вивчені власні стани електромагнітного поля в одновимірному фотонному кристалі, що містить дефектну пластину з шаруватого надпровідника. Ґрунтуючись на методі трансфер-матриці, з використанням електродинаміки джозефсонівської плазми, отримані дисперсійні співвідношення, які описують терагерцові електромагнітні моди, що локалізовані на дефекті. Розглядаються симетрична і антисиметричну конфігурації дефекту в фотонному кристалі. Порівняння дисперсійних спектрів локалізованих станів для надпровідного і діелектричного дефектів дозволило виявити особливості системи, що досліджується.

Ключові слова: фотонний кристал, трансфер-матриця, шаруватий надпровідник.